Structural analysis of a Vertical Axis Wind Turbine with a cylinder in the central axis

Catarina Correia Gonçalves
catarina.c.goncalves@tecnico.ulisboa.pt

Instituto Superior Técnico, Universidade de Lisboa, Portugal

December 2018

Abstract

Wind energy has benefited from a rising interest in the development of new and innovative solutions for harvesting wind power. Some projects have focused on harvesting wind from higher altitudes – the high-altitude wind energy systems. This thesis follows the design and development of a new wind turbine concept, which consists of applying the concept of a vertical axis wind turbine to an airborne module, based on the Magnus effect, already developed by *Omnidea*. This work will assess the viability of such a project. To start, a few concept ideas were compared in a concept screening process. Having the main design chosen, core parameters and values were analysed and chosen in order to maximize the efficiency. The next step was to design the mechanical components needed for the structure and define materials, attending to the importance of minimizing weight. For the system to float, the total weight of the structure and every part attached to the balloon could not weigh more than the buoyancy offered by the balloon – approximately 250 kg. After a design update, brought by the results of the finite element analyses, the total weight of the system rounded up to 264 kg. This could be addressed by creating a new module with higher length; or adding a smaller balloon to the existing one that could provide extra buoyancy.

Keywords: Wind turbine, VAWT, airborne wind system, Magnus effect, composite materials

1. Introduction

This study centres around the evolution and performance assessment of the existing prototype of a High-Altitude Wind Energy (HAWE) system developed by *Omnidea*, a Portuguese company which develops research in aerospace technology and energy systems. The current prototype is comprised of a lighter-than-air airborne module – a balloon filled with helium – with a cylindrical shape (currently with $3.8\,m$ in diameter and $18\,m$ in length) which reaches high altitudes (> 500m) by means of the Magnus Effect [1]. A small electric motor, mounted on the cylinder, is powered from a ground station and transmits rotation to the balloon, creating the necessary flow which, in addition to the incident wind, generates the necessary lift for the module to take flight. The ground station is equipped with a control system and a motor/generator to which the captured wind power is transferred. A tether cable is used to connect the two.

Presently, this HAWE system can serve as an observation or surveillance platform that can carry payloads. It can be used for terrain observation and/or mapping or for

telecommunications, as a signal receiver or extender. Another purpose, which is in focus here, is its capability to produce energy. The power production is performed by the ascending (production phase) and descending (recovery phase) movements of the module. When the operating altitude is reached, between these two phases, the rotation is ceased, the aerodynamic lift reaches zero and the energy needed for recovery is reduced. When the original position is reached the rotation is restarted and a new cycle begins.

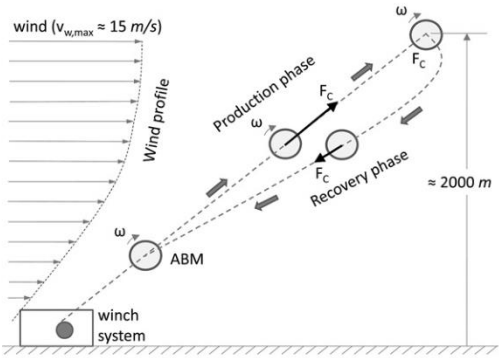

Figure 1 Schematic view of the concept based on the Magnus effect [2]

This process produces power in a discontinuous cycle, through a production and recovery phase, where there is no energy generation, only consumption (though in a small amount). For the cycle to be effective there must be a surplus of energy left after the recovery phase.

The new project aims to change the way the platform produces power. The airborne module would integrate a turbine structure, based on vertical axis wind turbines (VAWT), and the generator would move from the ground to the platform, thus allowing it to stay afloat for longer periods of time and to produce energy while it is at a fixed operating height instead of having to cyclically keep ascending and descending.

Through a concept development process, the specific VAWT system believed to be the best fit for the project at hand, was the H-Darrieus rotor model. This lift-type turbine is characterized by its straight vertical blades attached to the shaft through supporting arms. This concept will be applied to the existing airborne system, in a horizontal position, with its blades surrounding the balloon, with $R_{tur} > R_b$, in opposition to the having the blades at the side of the balloon with $R_{tur} = R_b$.

2. Wind power overview

Among the different renewable resources – solar, wind, hydro, biomass, etc. – wind energy, a practically endless source of energy, is found to be a cheaper alternative with a vast potential [3]. Nevertheless, even though vast, its distribution is not geographically uniform, and its availability is intermittent, both geographically and temporally. Still, significant progress has been made in the field of wind turbines and it has been found that altitude can be a determinant factor in wind availability. In higher altitude regions this influence is smaller, the wind becomes stronger and more consistent, with higher magnitudes. This introduces a new concept of high-altitude wind energy systems, working at heights of around $600\ m$, while typical terrestrial turbines work at $120\ m$ [4].

Wind turbines can be of one of two categories according to their axis of rotation: horizontal axis wind turbines (HAWT) or vertical axis wind turbines (VAWT). The latter have been found apt for generating electricity in conditions where HAWT's fail, for instance high wind speeds and turbulent wind flows. Due to their configuration VAWT's produce less noise, can harvest wind

from any direction and require no yaw system, which results in fewer power losses. On the downside, cyclic stresses can cause fatigue problems, they're often non-self-starting and have a larger blade area [3].

The maximum available power, for any kind of turbine is given by

$$P_{avail} = \frac{1}{2}\rho_\infty A V_\infty^3 \qquad (1)$$

Where ρ_∞ is the undisturbed air density, A is the area of the surface through which the wind passes and V_∞ is the undisturbed wind velocity. The efficiency of a wind turbine is characterized by the power coefficient

$$C_P = \frac{P_{rotor}}{P_{avail}} \qquad (2)$$

With P_{rotor} being the power generated by the turbine. The power coefficient is also related to the ratio between blade tip speed and wind speed, the Tip Speed Ratio (TSR)

$$TSR = \frac{\omega R_{tip}}{V_\infty} \qquad (3)$$

Where ω is the rotational speed of the turbine and R_{tip} is the radius of the blade tip, which in case of a VAWT equals the radius of the turbine R_{tur}.

Some researchers like Kirke [5] defined a range of design TSR instead of a single point. Specifically, a range where the power coefficient remains higher than 70% of $C_{P(max)}$ – Figure 2. This design range will serve as a reference for defining the main parameters of the turbine.

The rotational movement of the blades can be translated to a speed V_b, tangential to the revolving motion,

$$V_b = \omega\, R_{tur} \qquad (4)$$

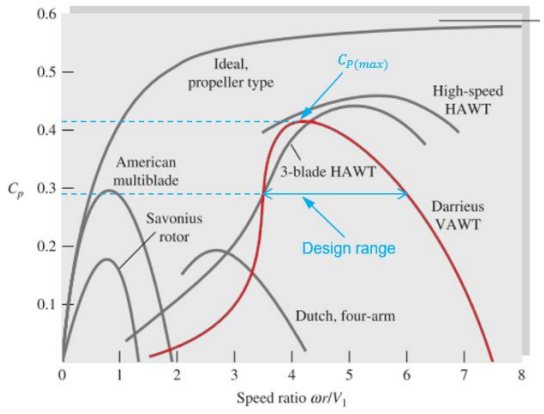

Figure 2 Estimated performance of various wind turbine designs as a function of blade tip speed ratio. Adapted from [6]

This means the air motion relative to the blade will be $-V_b$. This movement combined with a certain V_∞ results in each blade being subject to a relative velocity V_{rel}. This velocity vector changes magnitude and direction according to the blade's position θ, as in Figure 3.

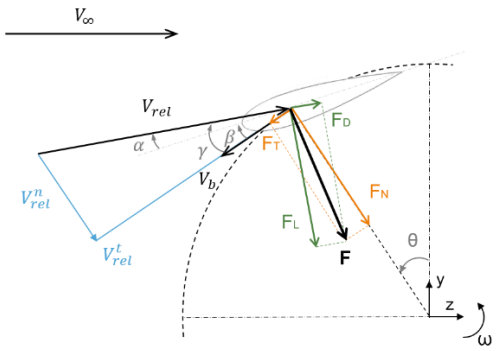

Figure 3 Definition of the force and velocity vectors. Adapted from [7]

From the tangential and normal components of V_{rel}, one gets

$$V_{rel} = V_\infty\sqrt{(TSR + \cos\theta)^2 + \sin^2\theta} \qquad (5)$$

The angle of attack, α, is a function of the input β, the blade incidence angle, and the blade's local angle of inflow γ. From Figure 3,

$$\gamma = \tan^{-1}\left(\frac{\sin\theta}{TSR + \cos\theta}\right) \qquad (6)$$

$$\alpha = \gamma - \beta \qquad (7)$$

This indicates that the angle of attack is not only a function of the blade's position θ but also of the tip speed ratio.

The net aerodynamic force on a single blade can be decomposed in two aerodynamic forces, lift F_L and drag F_D, perpendicular and tangential to the direction of the relative velocity, respectively. These are defined through the lift and drag coefficients, C_L and C_D, which depend on the Reynolds number, the angle of attack and the blade profile.

$$F_L = \frac{1}{2}\rho_\infty A_b V_{rel}^2 C_L \quad (8)$$

$$F_D = \frac{1}{2}\rho_\infty A_b V_{rel}^2 C_D \quad (9)$$

$A_b = c.L_b$ is the blade area, with c being the chord of the blade and L_b its length.

The net force F can also be decomposed in two other forces in the radial referential: F_N, the normal force, representing the structural loads on the blades, and F_T, the tangential force, represents the torque from the rotor [8]. These vectors can be expressed as a function of the aerodynamic forces and the local angle of inflow

$$F_T = F_L \sin\gamma - F_D \cos\gamma \quad (10)$$

$$F_N = F_L \cos\gamma + F_D \sin\gamma \quad (11)$$

Torque and power can be expressed as

$$T = F_T R_{tur} \quad (12)$$

$$P = T\omega \quad (13)$$

The average power for N_b number of blades, as a function of the position θ, can then be computed as

$$\bar{P} = \frac{N_b R_{tur}\omega}{2\pi}\int_0^{2\pi} F_T(\theta)d\theta \quad (14)$$

3. Conceptual Design and Parameters

The turbine will have fixed-pitch blades, which allow for a simpler, less expensive and more robust construction, and a variable speed rotor (the rotational speed is adjusted for an optimum point of operation considering the current wind speed). All its main conceptual parameters are defined in order to maximize the turbine's efficiency and lifting power.

A Weibull distribution was used to estimate the probability distribution of wind speeds at the site of functioning. The project team from *Omnidea* verified that the most frequent wind speed on the site of operation was $10\ m/s$ and the cut-in and cut-out speeds were set to 4 and $20\ m/s$, respectively.

3.1. Diameter and rotational speed

The tip speed ratio for a turbine as already been defined in equation (3). For simple spinning cylinders a ratio can be defined in the same way by substituting the radius of the turbine for the radius of said cylinder, designated spinning ratio. Sedaghat [9] developed a correlation for the lift to drag ratio, C_L/C_D, of rotating circular cylinders as a function of spinning ratio. The graph in Figure 4 shows this correlation and shows how C_L and C_D progress with spinning ratio individually.

The region with higher lift is in the region of greater spinning ratio; however, this is not the region with best performance, since it also means higher values of drag which can be unfavorable. Ergo, the optimum spinning ratio is a compromise between the two factors – higher lift and lower rotational speed. The value of optimum spinning ratio is estimated to be at the peak of the curve, where $X \approx 2$.

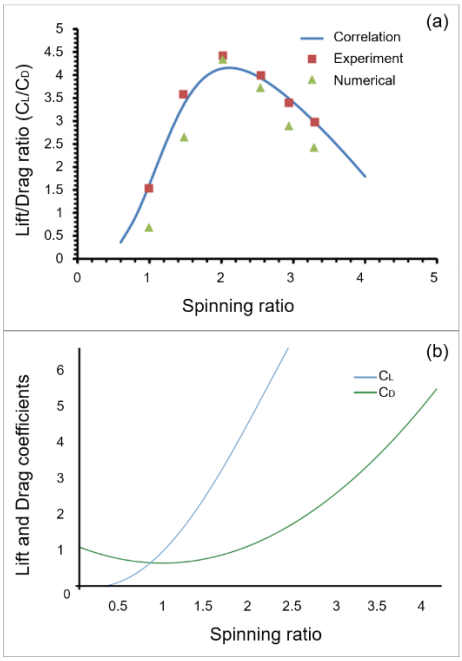

Figure 4 (a) Lift to drag ratio as a function of spinning ratio; (b) Lift and drag coefficients as a function of spinning ratio. [9]

From Figure 2, for a typical Darrieus VAWT, the maximum value for the power coefficient is found for $TSR \approx 4.2$. Therefore, for the same freestream wind speed, V_∞, knowing the diameter of the balloon and considering that both the balloon and the turbine will have the same angular velocity ω, it is possible to relate the two ratios and find the ideal turbine radius: $D_{tur} \approx 7.7\ m$. Knowing this, the rotational speed can be found for any wind velocity. The most pertinent cases are listed in Table 1.

Table 1 Rotational speeds for the rated and cut-out velocities

	$V\ [m/s]$	$\omega\ [rpm]$
Rated	10	104
Cut-out	20	124

3.2. Blade number

A balance between the turbine's aerodynamic efficiency and the blade's stiffness must be considered for determining the number of blades. Two- and three- bladed rotors are the typical choice due to their higher efficiencies [10] but there is a crucial difference between them: the net aerodynamic force acting on three-bladed rotors is steadier and less prone to sudden variation due to the position of the blades unlike two-bladed rotors.

3.3. Solidity and blade chord

Solidity is the measure of percentage of solid area in a circle traced by the rotor

$$\sigma = \frac{N_b c}{R_{tur}} \qquad (15)$$

Based on previous work [11] it is found that solidities between $0.3 < \sigma < 0.4$ lead to higher power coefficients. Allying a higher design range of TSR and a high $C_{P(max)}$ with the fact that higher solidity will mean more weight, the value of solidity chosen for this turbine will be $\sigma = 0.3$. From equation (15), the optimum blade chord is $c \approx 0.39\ m$.

3.4. Blade incidence angle

The blade's incidence angle β is a very important factor for performance enhancement since it relates to the angle of attack of the blade which can lead to an increase the lift, an important factor for the ability of flight of the balloon. From [10] it is possible to conclude that $\beta = -4°$ (out-offset) shows the highest value of $C_{P(max)}$ and the higher range of design TSR, making it a good choice for the turbine.

3.5. Blade profile

Only symmetrical profiles were considered as they do not need to readjust to wind direction since they produce aerodynamic lift from both sides of the aerofoil through a complete revolution of the rotor and have higher power output [11]. In particular, only NACA00XX profiles were considered. From [10], profiles with relative thickness of 15% and 18% have the highest lift-drag ratio indicating these as

preferred profiles. Larger thickness means higher blade stiffness and improves both the blade's ability to self-start and its power coefficient; it also means potentially more weight and a drag penalty. Nevertheless, the NACA0018 profile seems to be an appropriate choice for the turbine design.

3.6. Rated power and rotor length

One request from *Omnidea* was that the turbine should have a rated power between 10 and 20 kW. Since the balloon is 18 meters long, that should be the maximum permissible length for the turbine's blades. Wind is a variable source so, it is best to design the turbine for the most frequent wind velocity. Substituting equation (1) in (2) and defining the swept area A as $L_b D_{tur}$, the length can be calculated for any given wind speed

$$L_b = \frac{2P_{rated}}{C_P \rho_\infty D_{tur} V_{mf}^3} \qquad (16)$$

4. Mechanical design

4.1. Materials

Balloon net and guy wires - To provide stiffness and prevent the balloon from bending due to the ground tether cable force, *Omnidea* covered the balloon with a net made of high-modulus polyethylene (HMPE) rope – commercially, *Dyneema* – which will also be used for the guy wires.

Blades and support arms – the chosen material should combine the required structural properties to resist fatigue and centrifugal forces due to rotation, with low cost, low weight and the ability to be shaped into the selected aerofoil. Composite materials are considered the most appropriate since they show more favourable strength-to-weight ratios when compared to other materials. The manufacture of the blades will be handled by one of *Omnidea*'s partners, *UAVision*. Glass fibre, carbon fibre and Kevlar are three suitable choices for the composites' matrix; carbon fibre shows the best compromise between cost and mechanical properties adequate for the use case at hand.

A widely used lay-up is the quasi-isotropic laminate since, as the name indicates, it displays a behaviour close to isotropic. This is considered to be a reasonable solution for both the turbine blades and the support arms. A typical quasi-isotropic lay-up is the symmetric $[0/\pm 45/90]_s$, which has a minimum of eight layers.

Inserts – these parts are needed to attach the blades and support arms to each other and the support arms to the balloon. Metals are the most suitable material for the inserts due to their more uncommon and complex shapes, specifically aluminium alloys, which display favourable strength-to-weight ratios specifically of the 6000 and 7000 series, which are used by *Omnidea* (6063-T6 and 7075-T6, respectively). They can be bonded to the composite parts using specific adhesives.

4.2. Support arms design

The chosen cross-section of the arms was a non-lifting aerofoil profile designed by Eppler [12] for these kind of struts – the E864. The arms were placed at the ends of the blades, in order to minimize parasitic drag, despite the higher deflection when compared to overhang or cantilever supports. Since the balloon is not a rigid structure, placing a single arm as a support could lead the arms to force the balloon and rupture it. Therefore, arranging the arms in a triangle circumscribed about the balloon

(Figure 5) prevents the rupture by eliminating the forces in the radial direction and placing them only on the outer net, tangential to the balloon.

Guy wires are added to increase the stiffness of the structure, securing the sides of the blades to the rope that is casing the balloon.

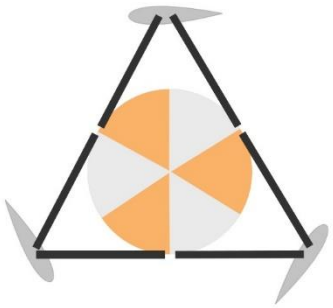

Figure 5 Configuration of the support arms

4.3. Generator and Drivetrain

The chosen generator must produce the necessary power mentioned in 3.6. If the generator is directly connected to the turbine there is no need for a gearbox which means fewer mechanical losses. However, lower speed generators, used for direct-drive, are heavier than their higher speed counterparts and so they are not viable for this project. Therefore, a generator with higher rotational speed must be chosen and, consequently, a drivetrain must be designed. From Alxion's website [13] the 300STK3M model was considered a suitable option, producing $12\ kW$ at a rated speed of $800\ rpm$.

4.4. Buoyancy and weight

The weight of the structure will influence how high the system can float before it needs to rotate in order to fly higher. This is given by the buoyancy of the balloon: it will float at a certain height, when the buoyant force is equal to weight of the structure. The volume of the balloon is equivalent to $250.84\ kg$ of air.

Table 2 Listing of weight of the structure's parts

Parts	**Weight [kg]**
Helium volume	34.07
Balloon net and skin	70
Transmission assembly	19.45
Generator assembly	27.62
Blade and support arms inserts	4.85
Blades	42.66
Support arms	26.16
Other parts	21.75
Total	**246.56**

Knowing the cable has a weight of $0.35\ kg/m$, this means the balloon can reach a floatation ceiling of about $12\ m$ until reaching the maximum allowed floatability.

4.5. Acting Loads

The loads acting on a blade, considered in this paper, are illustrated in Figure 7. They can be distributed along its length by dividing them by L_b.

Aerodynamic loads – it is known these are dependent on the environment conditions, which vary with time. As so, more than one load case should be considered when designing a turbine:

- **Load Case A** – normal operating conditions (V_{rated});
- **Load Case B** – maximum operating conditions ($V_{cut-out}$).

In the particular case of this turbine, if it reaches the maximum operating conditions it will be stopped and brought down for safe keeping; this way, load case B will lead the structural design of the turbine while load case A will only be monitored. In every case the loads are calculated as illustrated in Figure 6.

Centrifugal loads – these are directed outward, in a rotating reference frame. For a blade of

mass m subject to a rotation ω this force is given by

$$F_c = mR_{tur}\omega^2 \quad (17)$$

Gravitational Loads – are based on Newton's second law of motion

$$W = mg \quad (18)$$

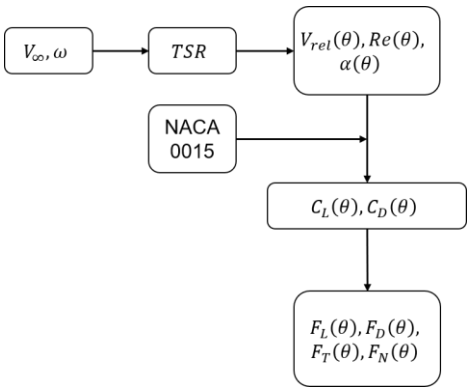

Figure 6 Load calculation flowchart

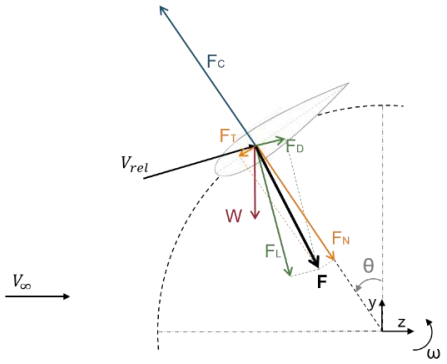

Figure 7 Total forces acting on a blade

For the support arms, only the maximum load case was considered, as their cross-section is not always in the same plane as the direction of the wind and only a computational fluids dynamic study would provide the necessary information on the actual variation of the aerodynamic forces and the influence of each arm on the others. The loads were calculated using a process similar to the blades.

4.6. Safety factors

The method of the partial safety factors as stated in [14] contemplates the uncertainties and variability in loads and materials, the uncertainties in analysis' methods and the importance of structural components with regard to the consequences of failure. For this, two partial safety factors are defined: for loads γ_F; for materials γ_M. The strategy is to turn the characteristic values of the forces, F_k, into design values, F_d, with which the stresses are calculated, $S(F_d)$. These are then compared to the design strength, computed from its characteristic value.

$$F_d = \gamma_F F_k \quad (19)$$

$$R_d = \frac{R_k}{\gamma_M} \quad (20)$$

$$S(F_d) \leq R_d \quad (21)$$

5. Finite Element Analysis

SolidWorks was used to model the turbine which was then imported to *Siemens NX* in order to perform the pre-processing of the model by simplifying, de-featuring and preparing the geometry for analysis in *NX Nastran*. It is also employed in the post-process and analysis of the computed results.

For the composite materials, the failure theory used was the maximum strain theory, where ply failure occurs when any principal material axis strain components exceed the corresponding ultimate strain.

5.1. Single blade simulations

A single blade was analysed in first place, for the situation of maximum load, so as to assess the performance of the component and the need for extra supports along its length. After the first analysis, it was found that the efforts on the blade surpassed the design strength by, approximately, 190%. For this reason, a few design options were simulated in order to find

Table 3 Results of the iterations simulations

# Iteration	1	2	3	4	5	6	7
Blade weight [kg]	14.20	14.75	17.19	27.75	14.57	18.73	14.20
Max displacement B [mm]	583	616	594	314	437	282	49
Max PFI B	1.601	1.738	1.701	0.916	1.417	1.116	0.451
Max ply strain 11 B	0.0113	0.0129	0.0120	0.0069	0.0112	0.0039	0.0031
Max ply strain 11 A	0.0079	0.0082	0.0073	0.0042	0.0069	0.0023	0.0019

the best configuration for the blades. In these iterations, the shear webs pattern was varied (2 and 3); the skin thickness was increased (4); a different profile, with higher thickness was tested (5); solidity was increased (6); and a third support was added to the initial configuration mid-length. The results are listed in Table 3. This study concluded that only the configuration from iteration 7 proved to be adequate for the load cases considered. As such, the turbine structure was redesigned in order to accommodate a third set of support arms.

5.2. Support arms

The support arms were also tested in order to reach the appropriate support arm chord length.

This happens when all three conditions of the maximum strain theory are met. The chord length achieved was $c = 110\,mm$. The evolution of maximum ply strain is detailed in Table 3. The minimum values are approximately symmetric, so they are not presented here.

Table 4 Results for the different support arms' chord simulations

Chord [mm]	Max ε_{11}	Max ε_{22}	Max ε_{12}
97.5	0.00446	0.00237	0.00434
100	0.00397	0.00151	0.00359
110	0.00386	0.00149	0.00257

5.3. Full structure

After analysing the blade's behaviour and verifying the support arms design, the full turbine structure was be simulated. The applied loads vary with different values of θ in order to simulate different orientations of the turbine with respect to the wind flow direction

The results proved to stay within the limits of the conditions of the maximum strain theory. Specific areas of the blades register values outside of the defined acceptable limits; this happens at the blades' extremities where the shear webs and blade covers meet. This issue is caused by the simplification of the model and it can be resolved by applying a reinforcement to the shear web, making it into an I-profile.

6. Conclusions

The purpose of *Omnidea*'s project was to develop a wind turbine that could be attached to the Magnus balloon system, in order for it to work at high altitudes where higher wind speeds are available and occur more often.

A concept development process was employed so as to first achieve the best concept idea for design. The main design parameters were compared and selected with the purpose of ensuring maximum efficiency. The mechanical components were designed to ensure structural integrity and to be as lightweight as possible.

This was the main difficulty in the project since the balloon only has so much buoyancy and the structure, besides lightweight, must be robust.

The balloon, besides providing the system with floatability, also has a role in providing lift. The Magnus effect will most likely be disturbed by the presence of the turbine, which is probably the main source of lift during rotation, but only a computational fluid dynamics study could provide more insight into that issue. This kind of study could also provide more accurate information on the amount of power the designed structure can produce which may affect the design of the blades and even the support arms of the turbine.

After the first structural finite element analyses, the rotor suffered some design changes which greatly affected the total weight of the structure, rounding it up to 264 kg. This could be addressed by creating a new module with higher length; or adding a smaller balloon to the existing one that could provide extra buoyancy.

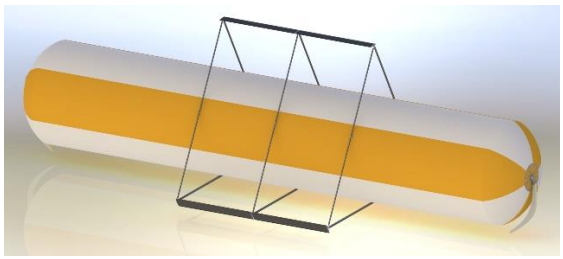

Figure 8 Render of the final design

7. References

[1] P. M. Oliveira, "Sustentação Aerodinâmica," 2008.

[2] R. Schmehl, *Airborne Wind Energy 2011*. 2011.

[3] M. M. Aslam Bhutta, N. Hayat, A. U. Farooq, Z. Ali, S. R. Jamil, and Z. Hussain, "Vertical axis wind turbine - A review of various configurations and design techniques," *Renew. Sustain. Energy Rev.*, vol. 16, no. 4, pp. 1926–1939, 2012.

[4] L. Perkovic, P. Silva, M. Ban, N. Kranjcevic, and N. Duic, "Harvesting high altitude wind energy for power production: The concept based on Magnus' effect," *Appl. Energy*, vol. 101, pp. 151–160, 2013.

[5] B. K. Kirke, "0 Evaluation of Self-Starting Vertical Axis Wind Turbines For Stand-Alone Applications," 1998.

[6] F. White, "Fluid Mechanics," *McGraw-Hill,New York*, 2010.

[7] M. Rossander *et al.*, "Evaluation of a blade force measurement system for a vertical axis wind turbine using load cells," *Energies*, vol. 8, no. 6, pp. 5973–5996, 2015.

[8] E. Dyachuk, M. Rossander, A. Goude, and H. Bernhoff, "Measurements of the aerodynamic normal forces on a 12-kW straight-bladed vertical axis wind turbine," *Energies*, vol. 8, no. 8, pp. 8482–8496, 2015.

[9] A. Hably, J. Dumon, and G. Smith, "Control of an airborne wind energy system with a Magnus effect," *Proc. Am. Control Conf.*, vol. 2016–July, no. May, p. 7, 2016.

[10] Y. -b. Liang, L. -x. Zhang, E. -x. Li, X. -h. Liu, and Y. Yang, "Design Considerations of Rotor Configuration for Straight-Bladed Vertical Axis Wind Turbines," *Adv. Mech. Eng.*, vol. 6, p. 16, 2015.

[11] M. Ahmadi-Baloutaki, R. Carriveau, and D. S.-K. Ting, "Straight-bladed vertical axis wind turbine rotor design guide based on aerodynamic performance and loading analysis," *Proc. Inst. Mech. Eng. Part A J. Power Energy*, vol. 228, no. 7, pp. 742–759, 2014.

[12] R. Eppler, *Airfoil Design and Data*. Springer-Verlag Berlin Heidelberg, 1990.

[13] Alxion, "STK Wind and water turbines alternators." [Online]. Available: http://www.alxion.com/products/stk-alternators/. [Accessed: 25-May-2018].

[14] Germanischer Lloyd Industrial Services GmbH, *Guideline for the Certification of Wind Turbines*. 2010.